NASA Technical Memorandum 110386

Optimization Study of the Ames 0.5" Two-Stage Light Gas Gun

D. W. Bogdanoff, Thermosciences Institute, Ames Research Center, Moffett Field, California

March 1996

National Aeronautics and
Space Administration

Ames Research Center
Moffett Field, California 94035-1000

Optimization Study of the Ames 0.5" Two-Stage Light Gas Gun

D. W. BOGDANOFF*

Thermosciences Institute

Ames Research Center

Summary

There is a need for more faithful simulation of space debris impacts on various space vehicles. Space debris impact velocities can range up to 14 km/sec and conventional two-stage light gas guns with moderately heavy saboted projectiles are limited to launch velocities of 7–8 km/sec. Any increases obtained in the launch velocities will result in more faithful simulations of debris impacts. It would also be valuable to reduce the maximum gun and projectile base pressures and the gun barrel erosion rate. In this paper, the results of a computational fluid dynamics (CFD) study designed to optimize the performance of the NASA Ames 0.5" gun by systematically varying seven gun operating parameters are reported. Particularly beneficial effects were predicted to occur if (1) the piston mass was decreased together with the powder mass and the hydrogen fill pressure and (2) the pump tube length was decreased. The optimum set of changes in gun operating conditions were predicted to produce an increase in muzzle velocity of 0.7–1.0 km/sec, simultaneously with a substantial decrease in gun erosion. Preliminary experimental data have validated the code predictions. Velocities of up to 8.2 km/sec with a 0.475 cm diameter saboted aluminum sphere have been obtained, along with large reductions in gun erosion rates.

I. Introduction

There is a need for more faithful simulation of space debris impacts on various vehicles, such as the space station, the shuttle, Earth and planetary entry and ballistic missile interceptors. Space debris impact velocities can range up to 14 km/sec and conventional two-stage light gas guns with projectiles with L/D ratios of 0.5–1.0 or larger, are limited to launch velocities of 7-8 km/sec (ref. 1). Any increases obtained in the launch velocities will result in more faithful simulations of debris impacts. In addition, it would be valuable, even while maintaining the same launch velocity, to improve gun component life and increase the likelihood of successful launches of the test package. This could be done by reducing the maximum gun and projectile base pressures and reducing the gun erosion rate.

There are a number of gun operating parameters which can be changed to attempt to reach these goals. Among the most important of these are:

1. Gunpowder mass.
2. Pump tube piston mass.
3. Break valve (diaphragm) rupture pressure.
4. Initial hydrogen fill pressure.
5. Length of pump tube.
6. Angle of high pressure contraction section.
7. Projectile mass.
8. Powder burn rate.

A number of earlier gun optimization studies have been conducted. In the work of reference 2, parameters 1, 2, 3, 4, and 7 above were varied (57 computational fluid dynamics (CFD) runs were made). Variation of the other parameters was not studied. Further, the degree of variations of parameters 2 and 3 in the work of reference 2 was somewhat limited (maximum variations of 27 percent and a factor of 3, respectively). There was also no study of the optimization of break valve rupture pressure while other parameters were also being optimized. The five optimization sweeps (each varying a single parameter) all passed through a single benchmark point; thus, multiparameter optimization was not done. In reference 3, parameter 6 is studied in some detail and some comparisons are made for two different powder burn rates and two different piston masses; i.e., a limited study was made of parameters 2 and 8 above. There is little or no discussion of optimization of the other parameters listed above. Further, the optimization work reported in reference 3 is aimed at somewhat lower muzzle velocities (5–6 km/sec) than those of interest herein (7–8 km/sec). Reference 4 is an earlier study at the Ames Research Center. All eight parameters listed above were investigated in that study, but the total number of CFD runs made (38) was rather small and therefore, the coverage of the parameter space was limited. In addition, the work of reference 4 shares the limitation of

*Senior Research Scientist.

reference 2 in that (1) optimization of break valve pressure was not considered while other parameters were optimized and (2) most optimizations passed through a single benchmark reference case while a single parameter was varied; thus, multiparameter optimization was not considered, for the most part.

We emphasize here that the earlier work referred to above is of high quality and has furnished a number of important results. The present work does allow us, however, to study areas not investigated by the earlier work as follows:

1. Seven of the parameters (all except for parameter 8) were investigated in the present study.

2. More CFD runs (77) were performed in the current study, allowing a more complete survey of the parameter space.

3. In the current study, considerable attention was paid to optimizing the break valve rupture pressure while other variables were being optimized.

4. The two main optimizations of the current study involve varying parameters 1, 2, 3, and 4 in sequence; thus a better degree of optimization is to be expected than for single-parameter optimizations around a single benchmark condition.

5. The current study uses an approximate correction for the erosion of wall material and the incorporation of this wall material into the hydrogen working gas. This is important for high muzzle velocity gun operating conditions and was not considered in the earlier studies.

The present CFD optimization was performed for the NASA Ames 0.5" gun. The effects of varying the gun parameters will be discussed in detail in the following sections.

Support for DWB by NASA (Contract NAS-2-14031) to Eloret is gratefully acknowledged.

II. CFD Code Description

The CFD code and its validation are described in detail in reference 5; hence, only a brief description of the code will be given here. The code is quasi-one-dimensional (quasi-1-D), uses the Godunov method and is third-order accurate in space and second-order accurate in time. The Riemann solver used is nearly exact. Friction and heat transfer to the tube wall for gases and dense media are modelled and a simple nonequilibrium turbulence model is used for gas flows. Realistic equations-of-state are used for all media. The code also models the gunpowder burn in the first stage breech.

The code was validated against a number of analytical solutions and by comparing its predictions against experimental data from the Ames 1.5" and 0.28" light gas guns, taken over a considerable range of gun operating conditions. The agreement between the CFD predictions and the experimental data was judged to be very good. Further details on the description and validation of the code can be found in reference 5.

III. Introduction to Survey

A. Gun Description and Benchmark Operating Conditions

Figure 1 is a sketch (not to scale) showing the benchmark configuration of the Ames 0.5" gun as modelled by the CFD code. Table 1 gives the benchmark operating conditions of the gun. The length of the pump tube can be defined in several ways, depending whether or not one wishes to include the volume of the piston and/or the contraction section or to give a volume-equivalent length. Hence, we do not give a specific length in table 1. However, from figure 1, the various ways of defining the pump tube length would yield values between 1549 and 1604 cm. The pump tube pistons are polyethylene rods, constructed with lands of slightly larger diameter at the forward and aft ends which ride on the pump tube wall. The lands are separated by a shank of slightly smaller diameter, which rides free of the wall during most of the piston stroke. The real piston has a Bridgeman seal at the forward end formed by machining a truncated conical hollow into the front face of the piston. This conical hollow cannot be modelled by the quasi-1-D CFD code. The equivalent 1-D piston set up in the CFD code has the same land lengths and shank diameters as the real piston and its length has been adjusted so that its mass is equal to that of the real piston. The land diameters of the 1-D piston have been reduced to be exactly equal to the pump tube bore diameter to allow for erosion of land material. Further details of piston modelling are given in reference 5.

B. Data Studied in Survey

The main data studied in evaluating the present survey are pressure histories at several different locations in the gun. For each gun firing cycle solution obtained, pressure histories were plotted at the following locations. (In the

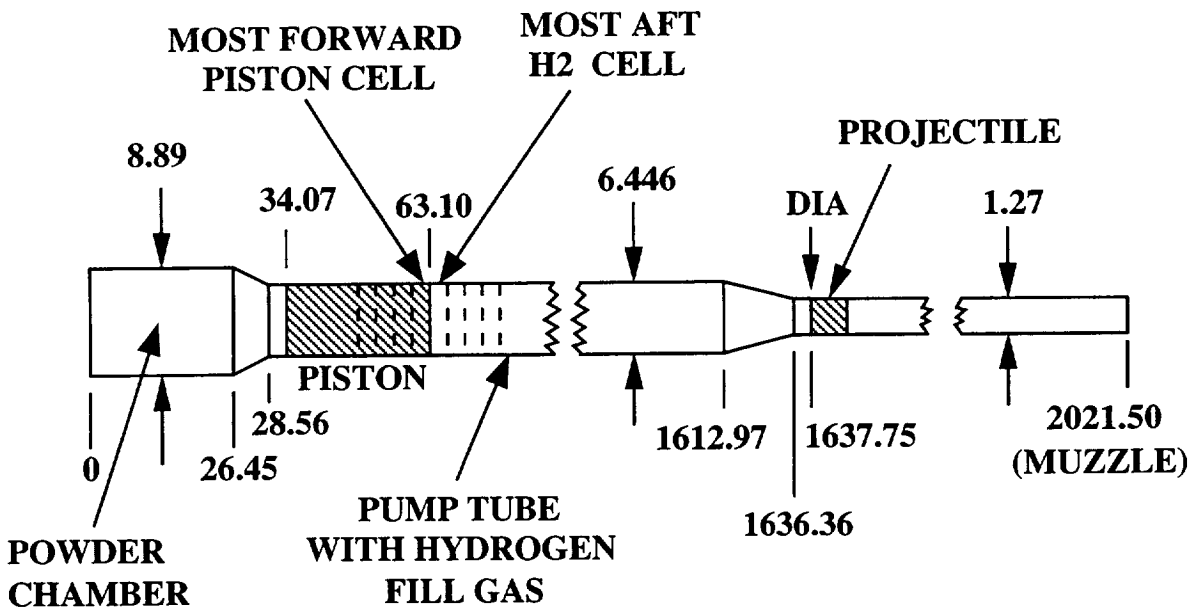

Figure 1. Gun modelled in CFD study. Not to scale. All dimensions are in cm. Numbers are distances from blind end of breech. DIA denotes diaphragm (break valve).

Table 1. Ames 0.5" gun benchmark operating conditions (gun parameter set #1)

Powder	IMR/DuPONT 4198
Powder mass	250 gm
Piston material	High-density polyethylene
Piston mass	904 gm
Pump tube hydrogen pressure	2.069 bar
Pump tube length	Benchmark, standard length
Break valve break pressure	345 bar
Sabot material	Lexan
Total launch mass	1.52 gm

list below, "forward" is in the projectile launch direction and "aft" is in the opposite direction.)

1. 15.587 cm aft of initial position of the projectile base.

2. 7.794 cm aft of initial position of the projectile base.

3. At the projectile base.

4. 6.64 cm forward of initial position of the projectile base.

5. Most forward cell in the moving grid which covers the piston.

6. Most aft cell in the moving grid which covers the hydrogen in the pump tube.

Positions 1 and 2 above are located at about 35 percent and 65 percent of the way along the high pressure contraction section for all cases except those with varying contraction section angle. Position 4 gives a measure of the maximum pressures which will occur in the barrel. Positions 1, 2, and 4 are fixed, while the remaining positions move with the motion of the projectile and piston.

Most of the discussion below will deal with the maximum pressures which occur at particular locations during the firing cycle, since these are critical for deformation and cracking of the gun and survival of the launch package. Examination of the pressure histories for all of the gun firing cycles studied to date has shown that most of the effects of changing gun operating conditions can be observed by examining the maximum pressures reached at the most forward position in the high pressure contraction section and at the projectile base (positions 2 and 3 listed above). The maximum pressures at the other positions are almost always either (1) very close to those at position 2 or (2) lie between those at positions 2 and 3. Hence, in the present paper, we will present maximum pressure data at positions 2 and 3 only.

Figure 2 shows calculated pressure histories at the projectile base and in the most forward cell in the pump tube hydrogen grid for the gun firing condition defined by "gun parameter set #2" given in table 2. Note the

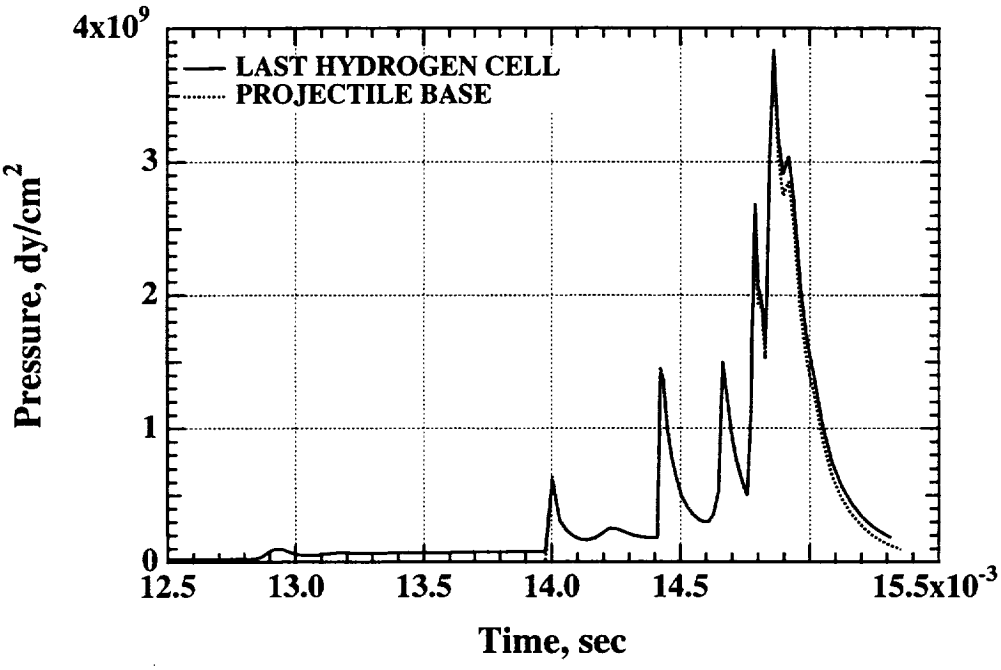

Figure 2. CFD pressure histories at the projectile base and at the most forward hydrogen cell for the gun firing conditions defined in table 2.

Table 2. Ames 0.5" gun benchmark operating conditions (gun parameter set #2)

Powder	IMR/DuPONT 4198
Powder mass	225 gm
Piston material	High-density polyethylene
Piston mass	723.31 gm
Pump tube hydrogen pressure	3.389 bar
Pump tube length	607.4 cm shorter than std. length
Break valve break pressure	300 bar
Sabot material	Lexan
Total launch mass	1.52 gm

succession of pressure peaks arriving at the projectile base. These are caused by shock waves reflecting between the front of the piston and the diaphragm or the projectile base. The sharp peaks, separated by valleys with much lower pressures, are caused by the shock wave focusing action of the conical high pressure contraction section. A very important concern in the present study is to predict the wave upon which the break valve (diaphragm) ruptures. For the case of figure 2 (with gun parameter set #2), the code predicts that the break valve will rupture on the wave at 14.0 msec. While varying gun operating parameters, such as powder mass or initial pump tube fill pressure, to obtain continuous curves, one must assure that break valve rupture continues to occur on the same wave as conditions are varied. In the present study, this was assured by varying the rupture pressure of the break valve as required. For the study of the effects of the variation of a number of gun operating parameters (e.g., powder mass, hydrogen fill pressure) in the present study, it was necessary, at times, to vary the break valve rupture pressure to ensure that the break valve was always rupturing on the most favorable wave.

The present paper represents a continuation of the work presented in reference 4. In addition to presenting an optimization of a different light gas gun than that discussed in reference 4, the present paper represents an advance over that previous work for reasons presented in the introduction. One of these reasons was the use, in the present paper, of a correction for the erosion of wall material and the incorporation of this material into the hydrogen working gas. This correction was obtained as follows. A rough correlation (shown in fig. 3) was made of experimental gun erosion data for the Ames 0.5", 1.0", and 1.5" guns. The four different symbols indicate individual data points from four data sets for the three different guns and the solid line is the trend line, estimated by eye, used in the estimation of the erosion correction. The correlation of figure 3 allows one to estimate the erosion in calibers per shot (at 4 calibers depth) as a function of (powder mass)/(barrel diameter)^3. [We note that a better correlation of gun barrel erosion has since been obtained and is presented in reference 7. This correlation correlates the gun erosion with both (powder mass)/(barrel diameter)^3 and (powder mass)/(hydrogen mass).] From the erosion

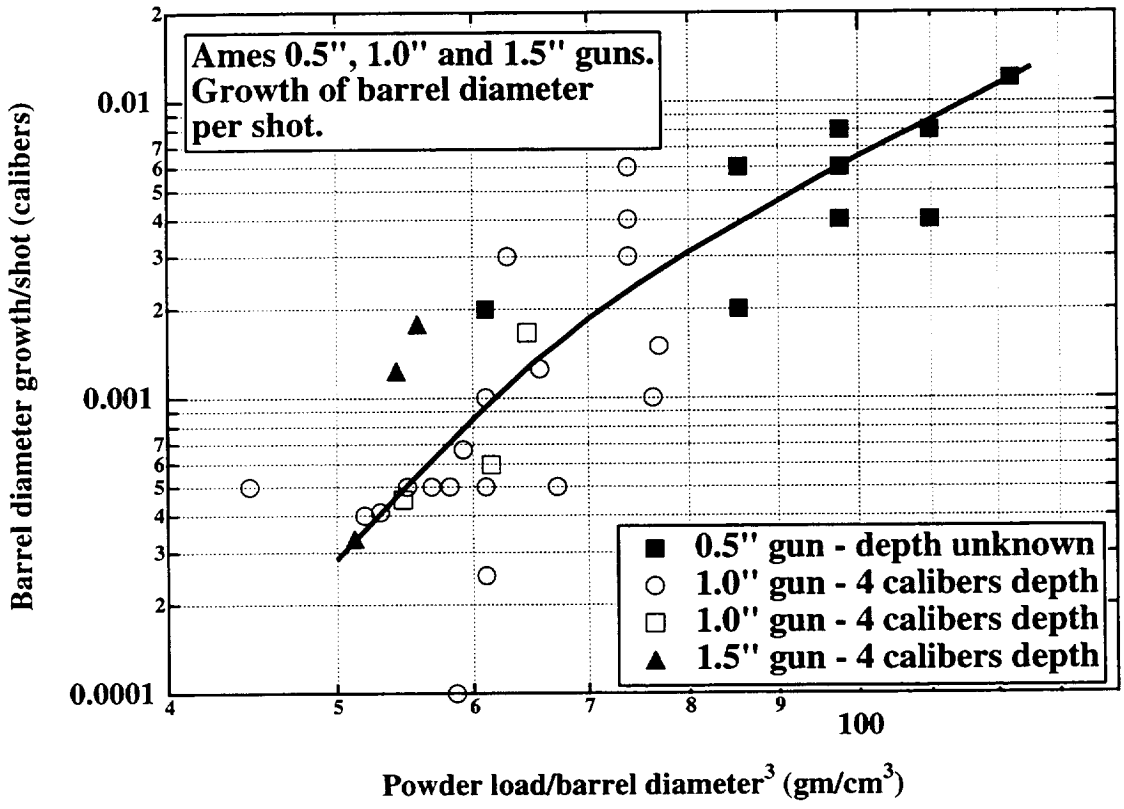

Figure 3. Experimental gun erosion data for the Ames 0.5", 1.0", and 1.5" guns plotted versus (powder mass)/(barrel diameter)^3. The four different symbols indicate individual data points from the four data sets and the solid line is the overall trend line.

estimate in calibers per shot, an estimate is made for the total barrel mass lost per shot, assuming that the erosion takes place uniformly over a length of 8 calibers. Based on measurements of the shapes of eroded gun barrels presented in reference 7, this gives a fairly good estimate of the actual amount of mass lost per shot. The initial mass of hydrogen in the pump tube can easily be calculated. To correct for the loading down of the hydrogen working gas with eroded gun material, the following correlation parameter was selected

$$\psi = \sqrt{\frac{\text{(Total working "gas" mass, i.e., hydrogen plus steel)}}{\text{(Hydrogen mass)}}}$$

CFD predictions were then made for five high velocity shots (up to 9.5 km/sec) with the Ames 0.5" light gas gun. The ratio

$$\beta = \frac{\text{(CFD prediction of muzzle velocity)}}{\text{(Experimental muzzle velocity)}}$$

was found to correlate fairly well with ψ. Figure 4 shows the velocity ratios, β, plotted versus ψ for these five high velocity shots (solid data points). The solid curve is the assumed trend curve for the erosion correction procedure. The curve was selected to pass through the two uppermost points and drops to $\beta = 1$ at the average ψ value for the three lowermost points. This correction was applied to all muzzle velocity results presented here. Below CFD muzzle velocities of about 7–7.5 km/sec, the correction procedure is not needed and the CFD code directly yields very good predictions of muzzle velocity (refs. 5 and 6). For high velocity shots, the correction can be substantial (see fig. 4). For example, for very severe launch conditions (high powder loads, low hydrogen pressures), the CFD predictions of muzzle velocities can be 12–13 km/sec, whereas the actual velocities achieved are 9–9.5 km/sec. The loading of the hydrogen gas by the eroded gun material is very severe in such cases. In 1996, it is hoped to modify the code to calculate gun erosion and the incorporation of the eroded material into the working gas. This would eliminate the need for the above correction procedure.

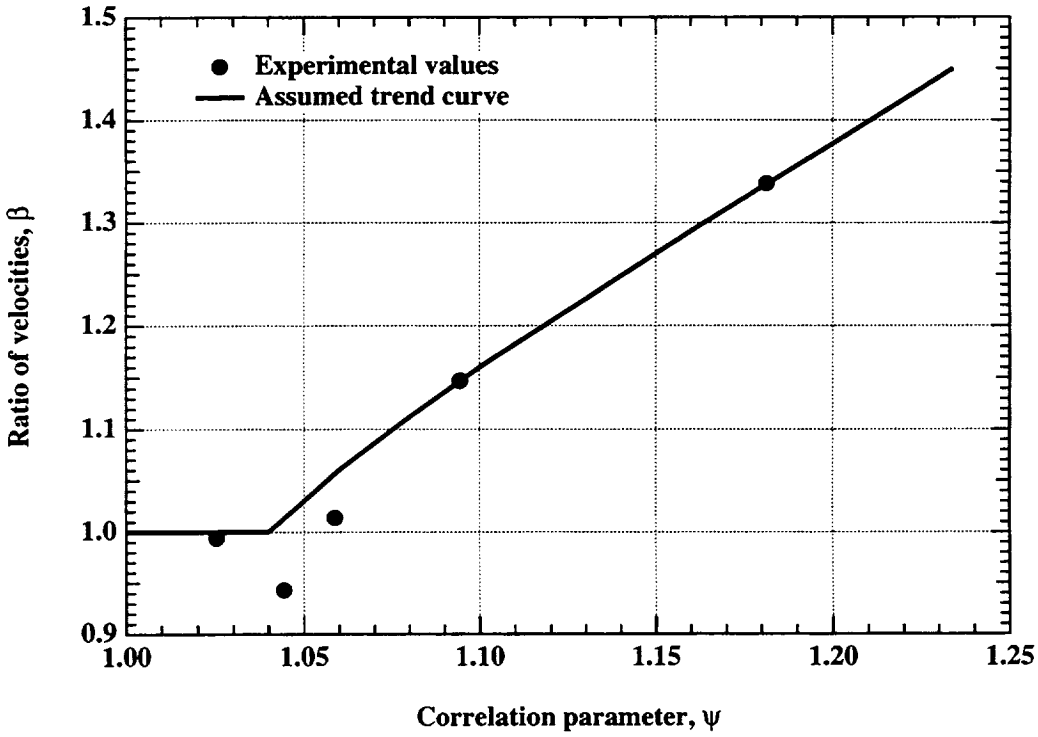

Figure 4. Muzzle velocity ratio, CFD/experimental, plotted versus the hydrogen mass–barrel erosion mass correlation parameter, ψ. Experimental data points (solid circles) are for five high velocity shots. The curve is the assumed trend curve for the erosion correction procedure.

IV. Convergence and Accuracy of CFD Results

Before beginning the discussion of the CFD surveys of the effects of changing the various gun operating parameters, we address the issues of convergence and accuracy of the CFD results. In this connection, several grid refinement studies have been performed for different gun operating conditions and have yielded very similar results for convergence and accuracy. Below, we discuss the most extensive of these surveys.

This survey was taken with the gun operating operating conditions defined by "gun parameter set #3," given in table 3. Table 4 shows the results of the grid refinement study. The gridding shown is the number of cells for the gunpowder/powder gas, piston and hydrogen zones, respectively. Looking at columns two to five, we can see that the solution is well converged for the finest grid, the difference between the pressures and velocities between the finest and second-finest grid being between 0.1 percent and 0.45 percent. Between the finest and the third finest grids, the corresponding differences range from 0.6 percent to 1.0 percent, except for the maximum contraction section pressure, for which the difference is 2.0 percent. To save CPU time, we have chosen to operate at the third finest grid shown. Hence, for the CFD results presented in this paper, the expected errors due to lack of complete convergence of the solutions would be 1 percent or less for the velocities and the maximum projectile base pressure and a maximum of about 2 percent for the maximum contraction cone pressure. This was judged to be sufficiently accurate for the present type of optimization survey.

For most of the results presented herein, however, there will be a somewhat larger error for the maximum projectile base pressure only. This error has nothing to do with lack of convergence of the solutions. To conserve disc space, only every 10th step is written in the final output files. Also, only every 10th step was examined to determine the maximum pressures. This limitation has virtually no effect on the piston or projectile muzzle velocities or on the recorded maximum value of the relatively slowly varying maximum contraction section pressures. It does have an effect on the recorded maximum projectile base

Table 3. Ames 0.5" gun benchmark operating conditions (gun parameter set #3)

Powder	IMR/DuPONT 4198
Powder mass	175 gm
Piston material	High-density polyethylene
Piston mass	723.31 gm
Pump tube hydrogen pressure	2.169 bar
Pump tube length	607.4 cm shorter than std. length
Break valve break pressure	500 bar
Sabot material	Lexan
Total launch mass	1.52 gm

Table 4. Grid refinement study for Ames 0.5" gun

Gridding	Muzzle velocity (km/sec)	Piston velocity[a] (m/sec)	Max. proj. base pressure (dy/cm^2)	Max. contr. cone press.[b] (dy/cm^2)	CPU time (sec)
6,6,22	7.689	796.8	3.642×10^9	11.30×10^9	191
8,8,30	8.132	809.7	4.318×10^9	13.43×10^9	324
10,10,38	8.075	800.4	4.185×10^9	13.26×10^9	502
14,14,52	8.215	804.6	4.352×10^9	14.05×10^9	939
16,16,56	8.165	798.9	4.290×10^9	13.82×10^9	1165
18,18,60	8.145	799.8	4.309×10^9	13.77×10^9	1406

[a]Between x = 930.5 cm and x = 942.6 cm along pump tube.

[b]At x = 1021.2 cm.

pressure, since a number of waves with very sharp peaks strike the base of the projectile. For the runs shown in table 4, the difference between the maximum projectile base pressure examining every timestep (as shown in the table) and that calculated examining every 10th timestep was 2–8 percent. For all the runs discussed herein, except those shown in table 4, only the maximum projectile base pressure based on examining every 10th timestep is available. The final assessment of the accuracy of the computational results presented herein is thus:

(a) Muzzle velocity–within 1 percent of converged value.

(b) Maximum pressure in contraction cone–within 2 percent of converged value.

(c) Maximum pressure at projectile base–solution is converged to within 1 percent, but quoted values are 2–8 percent low, since only every 10th step was sampled to obtain the maximum value.

The CPU times shown in table 4 are for single-processor calculations on a Cray C-90 machine. Typical CPU times for the 16,16,54 gridding are 600-950 sec. If vectorized, the code would likely run 10–100 times faster.

V. Survey of Gun Operating Conditions

A. Full Length Pump Tube

The first part of the survey involves operation of the gun with the full pump tube length shown in figure 1. We begin by running CFD solutions for a powder mass of 250 gm, a pump tube fill pressure of 2.069 bar and a total launch mass of 1.52 gm. The piston and projectile materials and the type of gunpowder are as shown in table 1. Solutions were run for five different piston masses. Figure 5 shows the maximum projectile base pressures versus muzzle velocity for all of these runs. For the solid curve with the solid data points, the piston mass in grams is shown underlined for each data point. For piston masses of 1130, 904, and 723 gm, solutions were run at two additional break valve rupture pressures to determine the optimum wave on which to rupture the break valve. For

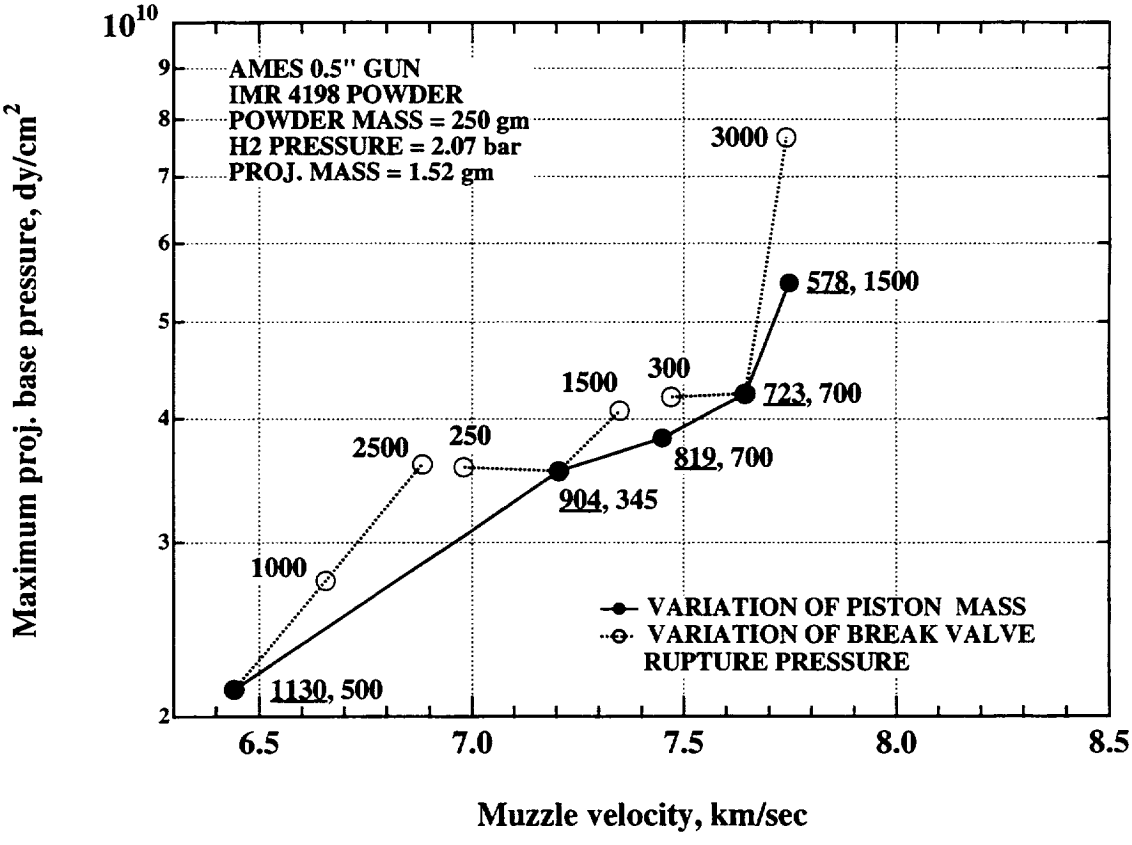

Figure 5. Maximum projectile base pressure versus muzzle velocity. Numbers beside data points are piston masses (gm), underlined, and break valve rupture pressure (bar).

each of these three piston masses, the results for the three different rupture pressures are shown joined by the dotted curve. Beside all data points, not underlined, is shown the break valve rupture pressure in bars. For the variation of piston mass and break valve rupture pressure only shown in figure 5, it is apparent that the solid line represents the most favorable operating condition of the gun. (One wishes always to move towards the lower right corner of the graph to obtain the most favorable operating conditions.) All of the operating conditions along the solid curve have the diaphragm rupture occurring on the same wave. It should be pointed out that the solid data points with piston masses of 904 and 1130 gm are representative of high performance gun operating conditions which have been used frequently in the past for projectile masses in the region of 1.5 grams.

Since one wishes to move towards the lower right corner of the graph, the bulge of the solid black curve in that direction (for piston masses of 819 and 723 gm) was selected as a starting point to vary two additional parameters. For a piston mass of 723 grams, the powder mass was varied from 275 to 175 gm, always keeping on the same wave for diaphragm rupture. Then, from the operating condition with a piston mass of 723 gm and a powder mass of 175 gm, the hydrogen fill pressure was reduced from 2.07 bar to 1.32 bar, again always keeping on the same wave for diaphragm rupture. The resulting curves of maximum projectile base pressure versus muzzle velocity are shown in figure 6. The upper solid curve of figure 6 is the same as the solid curve in figure 5. For clarity, in figure 6, we have omitted the curves showing the effect of varying the break valve rupture pressure which appear in figure 5. The break valve rupture pressures required to maintain rupture on the same wave were, for the points on the dotted curve (variation of powder mass), from top to bottom, 1000, 700, 700, 600, and 400 bar. For the points on the lower solid curve (variation of hydrogen fill pressure), the necessary break valve rupture pressures were, from left to right, 400, 400, 300, and 300 bar.

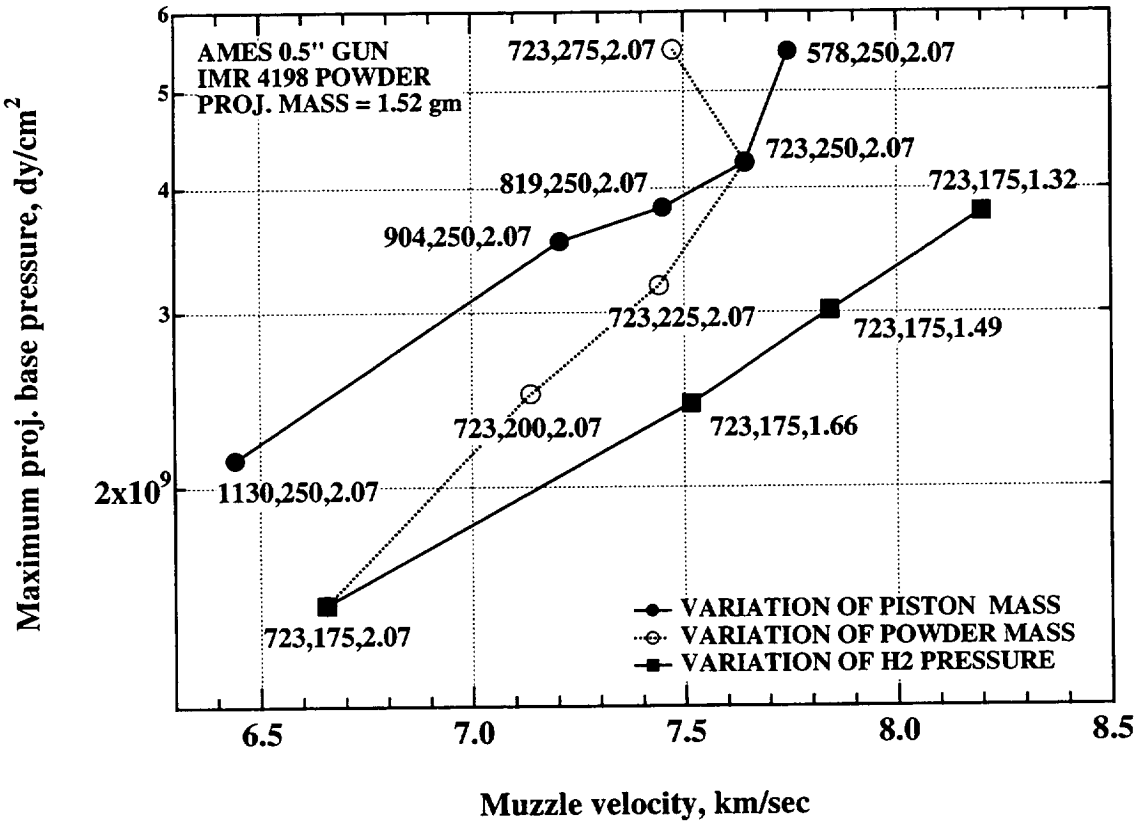

Figure 6. Maximum projectile base pressure versus muzzle velocity, showing the effects of varying piston mass, powder mass and hydrogen fill pressure. Numbers beside data points are piston masses (gm), powder masses (gm) and hydrogen fill pressure (bar).

From figure 6, it can be seen that moving from the more traditional gun operating conditions (lower two points along the upper solid curve) to the new conditions calculated along the lower solid curve entails very substantial advantages. For example, while maintaining a given maximum projectile base pressure, one may raise the muzzle velocity 0.8–1.0 km/sec. One may also choose to maintain the same muzzle velocity and achieve a 35–40 percent drop in maximum projectile base pressure. Further, simultaneously with making either one of these two changes, from our correlation of gun erosion versus powder mass, one should achieve a reduction in gun erosion of 50 percent or more.

One should examine whether the improved performance at the projectile base achieved from shifting from the upper to the lower solid curve in figure 6 might be accompanied by a deterioration in performance at other locations in the gun. To examine this issue, we present figure 7, which is a strict analog of figure 6, except that the ordinate now gives the maximum pressures at a point about 65 percent along the high pressure contraction cone of the gun. This location is known, from a number of previous studies, to be subjected to very nearly the maximum pressures which occur anywhere in the gun during any particular gun firing cycle.

We note that the maximum pressures occurring in the high pressure contraction cone are about 4 times those at the projectile base. Further, the improvement in shifting from the gun operating conditions represented by the upper solid curve of figure 6 to those represented by the lower solid curve (for the maximum projectile base pressure) is paralleled by a very similar improvement in the high pressure contraction cone. This was also found to be true for other locations in the gun for which data is not shown here. Thus, the improvement achieved by these suggested changes in gun operating conditions appears to apply to the entire area of the gun subject to high hydrogen pressures in rather similar (though not identical) ways. This was also found to be true for the second optimization presented in section V, part B. For this reason, we will present herein, from now on, plots of maximum projectile base pressure versus muzzle velocity only.

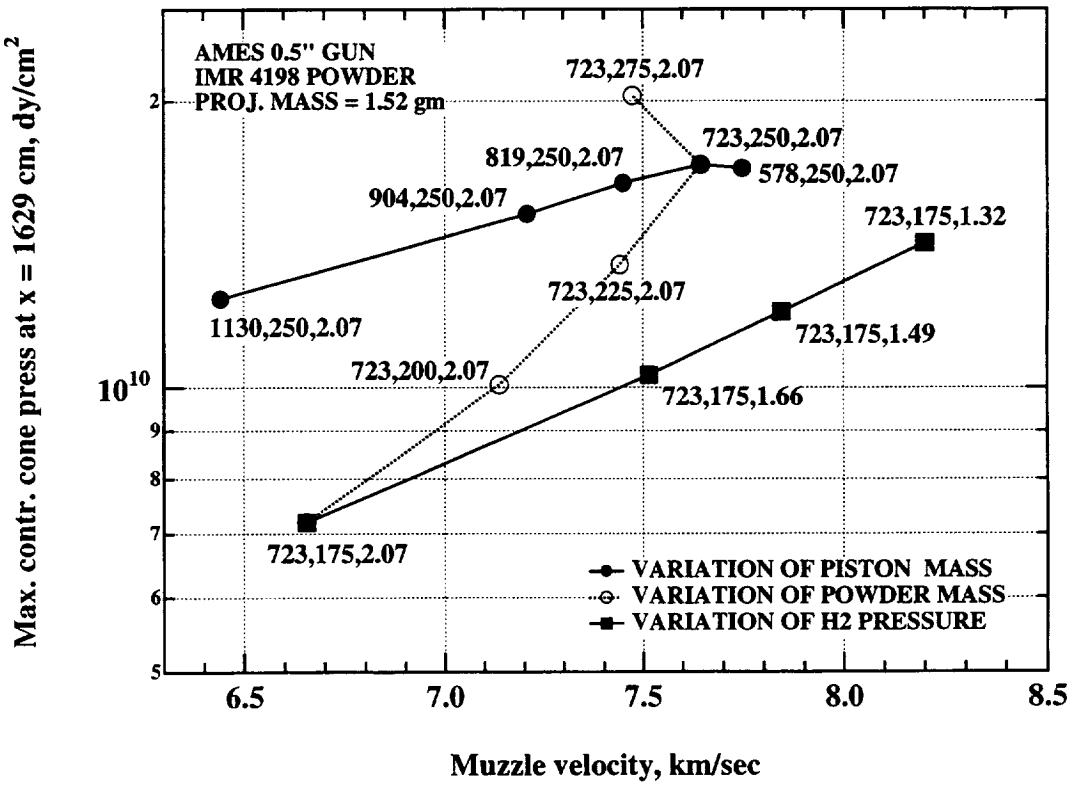

Figure 7. Maximum pressure at a point about 65 percent of the way along the high pressure contraction cone versus muzzle velocity, showing the effects of varying piston mass, powder mass and hydrogen fill pressure. Numbers beside data points are piston masses (gm), powder masses (gm) and hydrogen fill pressure (bar).

We now discuss the effect of reducing the projectile mass. We return to figure 6. Starting from the point on the uppermost curve for a projectile mass of 819 gm, a second set of optimizations, not shown here, was performed because a number of pistons of this mass were available. This second optimization involved, as for the data shown for 723 gm pistons, a reduction in powder mass from 250 to 175 gram, followed by a reduction in hydrogen fill pressure from 2.07 to 1.32 bar. The result was two curves which lie slightly above the dashed curve and the lower solid curve in figure 6. For the lowest curve for the 819 gram piston (powder mass of 175 gm, hydrogen fill pressures of 2.07 to 1.32 bar), the CFD analyses were then repeated for projectile masses of 1.31 instead of 1.52 gram. The results of the decrease of projectile mass from 1.52 gm to 1.31 gm were as follows.

1. Only very small increases in muzzle velocity (0–2 percent) were predicted to occur.

2. The maximum projectile base pressures were reduced roughly in proportion to the projectile mass.

3. The maximum pressure in the high pressure contraction cone was essentially unchanged.

Thus, the principal advantage in reducing the projectile mass for this type of gun operating condition appears to be the reduction in the maximum base pressure on the projectile.

B. Shortened Pump Tube

Because of the improved performance with a shortened pump tube observed for the Ames 1.5" light gas gun (ref. 4), a second optimization series was carried out on the Ames 0.5" gun with a shortened pump tube. A convenient joint between pump tube sections allowed 607 cm of pump tube length to be removed, reducing the pump tube volume by about 40 percent. For the optimizations described here, the hydrogen pressures were correspondingly increased, so that the total amount of hydrogen gas in the pump tube was the same for corresponding cases with the full pump tube length and with the shortened pump tube. The optimizations now to be discussed will follow very nearly the same sequence used in section V, part A for the optimization for the full length pump tube.

Figure 8 shows, for the shortened pump tube, the maximum projectile base pressure plotted versus muzzle

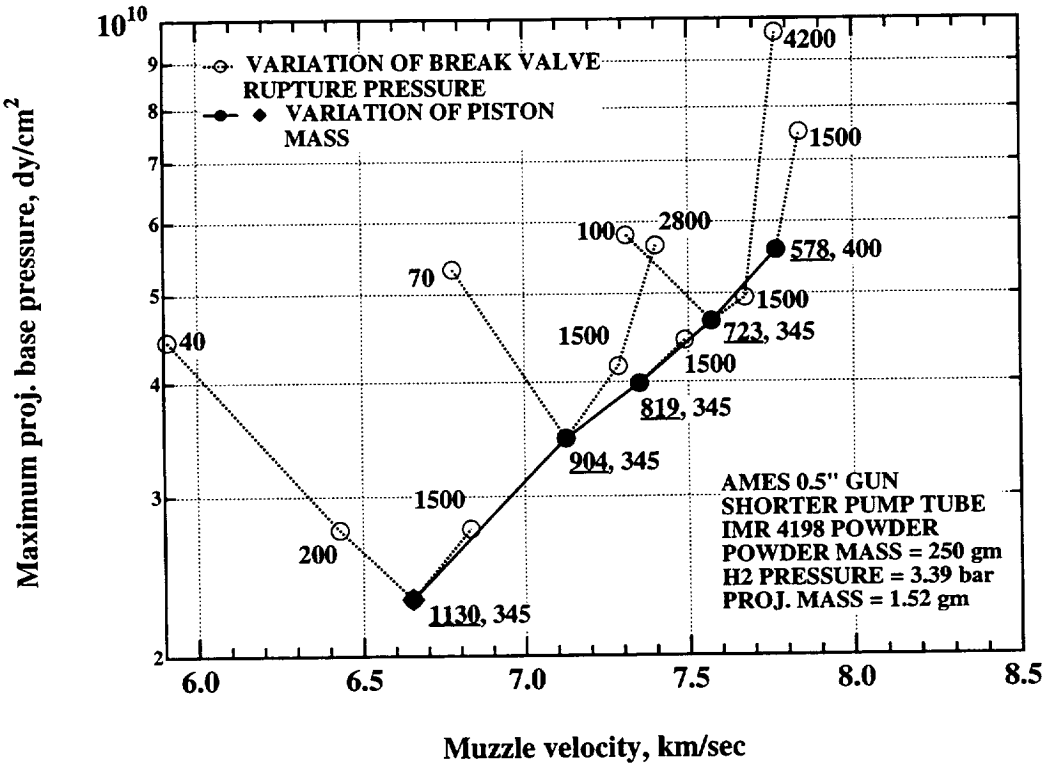

Figure 8. Maximum projectile base pressure versus muzzle velocity for the shortened pump tube. Parameters varied are piston mass and break valve rupture pressure. Numbers beside data points are piston masses (gm), underlined, and break valve rupture pressure (bar).

velocity, showing the effects of varying piston mass and break valve rupture pressure. This figure is closely analogous to figure 5 for the case with the full length pump tube. More CFD runs were made to obtain the data shown in figure 8 than for that shown in figure 5. This allowed the effect of varying break valve rupture pressure to be more completely defined. In figure 5, for each of three piston masses, three rupture pressures were investigated. For the remaining two piston masses, only a single rupture pressure was investigated. In contrast, in figure 8, for each of three piston masses, four rupture pressures were investigated and for the remaining two piston masses, two rupture pressures were investigated. For each of the piston masses for which four rupture pressures were investigated, the four cases studied correspond to break valve rupture on one of 4 successive waves arriving at the projectile base. For all three of these cases, it is the same four waves which arrive in succession at the projectile base. For the piston masses for which only two rupture pressures were investigated, this corresponds to rupture on the second and third waves of the four discussed above.

The solid line with solid data points in figure 8 shows the envelope of the optimum gun operating conditions based on variation of piston mass and break valve rupture pressure only. For the four lowest piston masses, the best wave on which to rupture the break valve is the second wave (solid circular data points), except that the condition for the 723 gram piston with rupture on the third wave is very slightly better than the envelope for rupture on the second wave. However, for the 1130 gram piston, it is clear that rupture on the third wave produces a significantly better operating condition. This point is indicated by the solid diamond data point. Thus, between piston masses of 904 and 1130 grams, the optimum wave on which to rupture the break valve changes from the second wave to the third wave. Thus, careful attention to the selection of the wave upon which the break valve will rupture is critical in the optimization of gun operating parameters.

The next part of the optimization follows that which was done for full length pump tube in section V, part A. Starting from the solid data point in figure 8 for a piston mass of 723 gm, the powder mass was reduced to 175 gm. Then, the hydrogen fill pressure was reduced from 3.39 to 2.17 bar. For the powder mass variation, the break valve rupture pressure was adjusted to maintain the rupture on the second wave. For the hydrogen fill pressure variation, runs at each hydrogen pressure were made with break valve rupture occurring on several different waves. In this case, for all hydrogen fill pressures investigated, it was found that break valve rupture on the third wave gave the best performance. Again, this points out the necessity of paying close attention to the selection of the wave on which the break valve rupture while optimizing operation of the gun. The results of these calculations are shown in figure 9. The uppermost solid curve is the solid curve shown in figure 8. The curves showing the effect of varying the break valve rupture pressure in figure 8 are

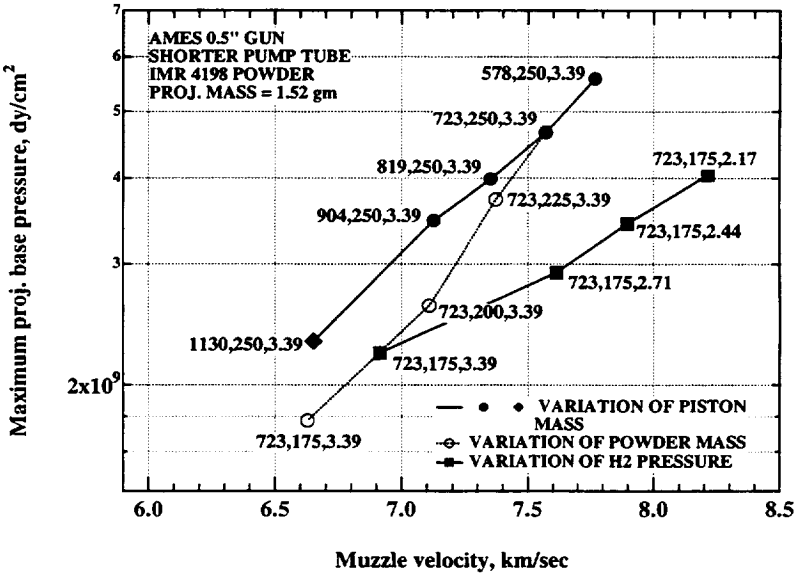

Figure 9. Maximum projectile base pressure versus muzzle velocity, showing the effects of varying piston mass, powder mass, and hydrogen fill pressure. Numbers beside data points are piston masses (gm), powder masses (gm), and hydrogen fill pressure (bar).

omitted in figure 9 for clarity. The dotted curve is the curve for the variation of powder mass; for this curve, break valve rupture always occurs on the second wave. The lower solid curve is the curve for the variation of hydrogen fill pressure and, for this curve, break valve rupture always occurs on the third (and optimum) wave. The break valve rupture pressures required to maintain rupture on the same wave were, for the points on the dotted curve (variation of powder mass), from top to bottom, 250, 250, 150, and 150 bar. For the points on the lower solid curve (variation of hydrogen fill pressure), the necessary break valve rupture pressures were, from left to right, 600, 600, 500, and 500 bar.

The gains achievable in moving from the upper to the lower solid curves in figure 9 are very similar to those which were noted from figure 6 in section V, part A for the full length pump tube. For example, while maintaining a given maximum projectile base pressure, one may raise the muzzle velocity 0.7–0.9 km/sec. One may also choose to maintain the same muzzle velocity and achieve a 30-40 percent drop in maximum projectile base pressure. Further, simultaneously with making either one of these two changes, from our correlation of gun erosion versus powder mass, one should achieve a reduction in gun erosion of 50 percent or more.

C. Comparison of CFD and Experimental Results

Before starting the CFD-experimental discussion proper, we make a comparison of the final optimized curve for the full length pump tube (taken from fig. 6) with the corresponding curve for the shortened pump tube (taken from fig. 9). These two curves are shown in figure 10 below. It is immediately apparent from figure 10 that the optimization with the full length pump tube appears to be slightly superior to that for the shortened pump tube. Hence, one may well ask: why shorten the pump tube? The answer has to do with the correction applied to the initial CFD results (which do not, yet, model gun erosion) to allow for the effect of erosion of gun material and the incorporation of this high molecular weight material into the hydrogen

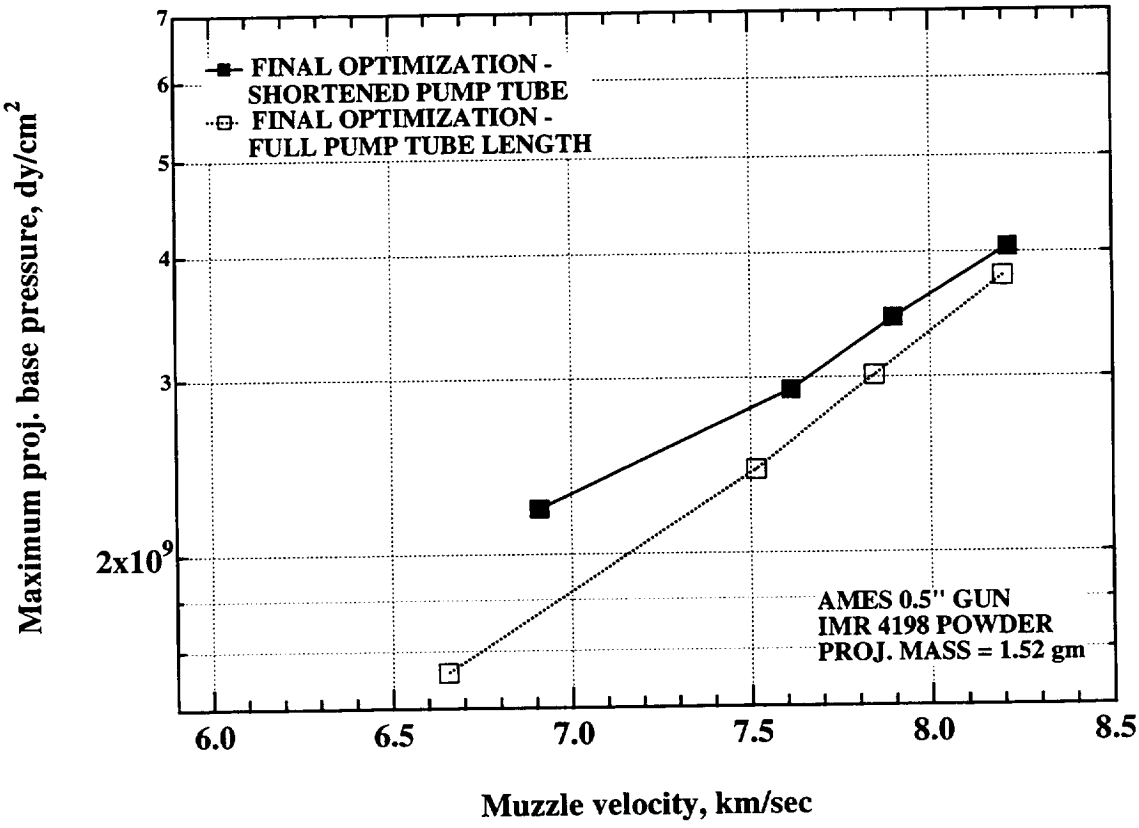

Figure 10. Final optimized curves of maximum projectile base pressure versus muzzle velocity, for the full length and shortened pump tubes. Curves taken from figures 6 and 9.

working gas (see sec. III, part B). The actual gun erosion data is very difficult to acquire and has a large scatter (ref. 7), and therefore, to date, we have only been able to discern a definite correlation between gun erosion per shot and powder mass. It is clear that other variables (such as pump tube length) effect gun erosion, but we are not yet able to extract these effects from the very noisy gun erosion data. Thus, the relationship of the two lines shown in figure 10 is only roughly indicative and indeed, other experimental work (ref. 4) has shown that shortening the pump tube actually results in somewhat increased muzzle velocities and reduced gun erosion.

Before comparing the experimental and theoretical muzzle velocities, two issues will be addressed: (1) the accuracy of the experimental muzzle velocities and (2) the difference between the gunpowders used in the CFD solutions and in the experiments.

The experimental velocity data is obtained by observing the successive passage of the projectile through several sets of time gates. Projectile passage is detected by photomultiplier tubes or by a electrical contact being made upon impact. A correction must be applied for the deceleration of the projectile as it passes through the gas in the dump tank. Allowing for this deceleration, several different values are obtained for the projectile muzzle velocity because the projectile passes though several pairs of time gates. The average of these is the quoted value of the muzzle velocity. The scatter in these values gives a measure of the accuracy of the experimental muzzle velocities. For a large number of shots, the maximum total scatter of muzzle velocities is 0.5–0.6 percent. Thus, the accuracy of the quoted experimental muzzle velocities is very likely less than 0.3 percent and is certainly less than 0.6 percent.

The CFD calculations were made with IMR/DuPont 4198 powder, whereas the experimental firings used IMR/DuPont 4895 powder. Since these powders have significant differences in burn rates, this is an undesirable situation. In this paragraph, we discuss why this difference exists and why we believe that valid CFD/experimental comparisons can be made in spite of the two different powders. For reasons of availability, the 4895 powder was chosen for the 1995–96 work with the Ames 0.5" gun. All of the data on the Ames 0.5" gun from the 1960s onwards was examined and no powder chamber pressure data could be found for 4895 powder. Limited powder chamber pressure data for the 4198 powder was available, however. These two powders have essentially the same chemistry, but the grain sizes are significantly different, leading to significant differences in burn rates. Lacking any powder chamber pressure data for the 4895 powder, the powder burn rate and piston friction values to be used in the code were adjusted (see ref. 5, sec. 5.2) using the data for the 4198 powder. The parameter survey was then started. When 60 of the 77 CFD solutions had been obtained, the first shots were fired with the 4895 powder and powder chamber pressure for that powder was now available. It was immediately obvious that the powders burned in significantly different manner and that the 60 CFD solutions in hand were not directly applicable to the new experimental shot data now available. Since it is known that the key parameter is the piston velocity as it enters the high pressure contraction section, the following technique was developed. For a comparison between CFD and experimental results, all parameters correspond exactly except (1) type of powder, as discussed above and (2) powder mass. Basically, the powder mass in either the CFD calculation or the actual gun firing is adjusted so that the piston velocity between the last pair of whisker gauges before the contraction cone entrance is matched between theory and experiment. This technique allows the effectiveness of the experimental implementation of optimization survey to be evaluated. It is emphasized that this adjustment of powder mass is not done when powder chamber pressure data is available for the powder in question (refs 4–6).

Figure 11 shows the comparison of CFD and experimental muzzle velocity data for a limited set of experimental data. Shown are comparisons for four shots with the full length pump tube and three shots with the shortened pump tube. The gun operating conditions for all these shots were close to one or the other of the curves in figure 10. The projectile masses varied from 1.17 to 1.35 grams. It is seen that for the two lowest performance shots with the full length pump tube, the difference between the CFD and the experimental results is 1–2 percent. Moving from the two lowest performance shots to the intermediate performance shot (at an experimental muzzle velocity of 7.2 km/sec), by reducing the hydrogen fill pressure from 2.07 to 1.67 bar, the CFD predictions of muzzle velocity increase by 1.25 km/sec. The experimentally observed increase is substantial, 0.88 km/sec, but is about 30 percent smaller than the CFD value. When the hydrogen fill pressure was lowered a second time (from 1.67 to 1.32 bar, for the data point at an experimental muzzle velocity of 7.35 km/sec), very little further improvement in muzzle velocity was observed (only 0.19 km/sec), whereas the CFD calculations predicted a substantial further improvement (about 0.70 km/sec). This is believed to be due a large increase in gun erosion for the lowest hydrogen fill pressure which is not modelled by our simple correction technique. A similar phenomenon has been observed in the past with the full length pump tube. For example, for powder masses of 175 and 200 grams and projectiles weighing about 0.9 gm, very little muzzle

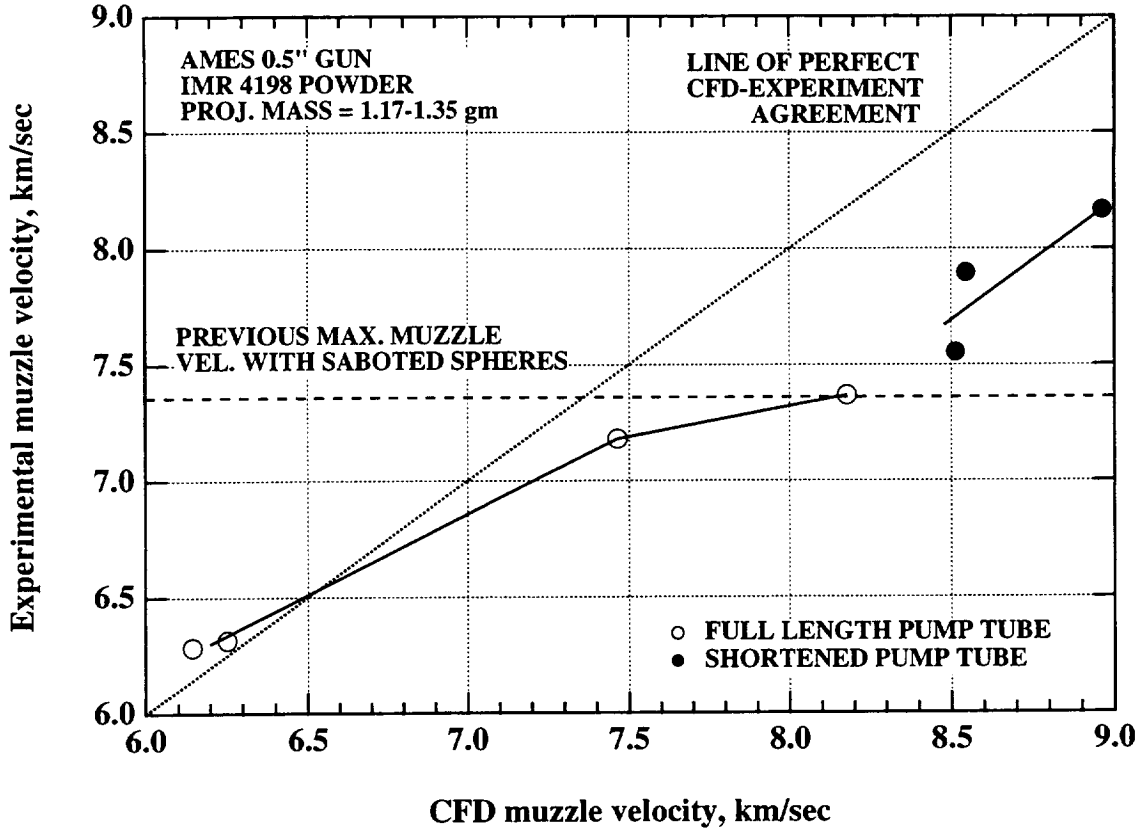

Figure 11. Experimental versus CFD muzzle velocities for the Ames 0.5" gun.

velocity increase (about 3 percent) was observed upon reducing the hydrogen fill pressure from 1.03 to 0.69 bar, whereas very much larger velocity increases were predicted by CFD calculations. For the three shots with shortened pump tube, we see that (1) higher muzzle velocities are obtained, ranging from 7.5 to 8.2 km/sec and (2) the experimental muzzle velocities continue to rise as the fill pressure is reduced from 2.17 to 2.05 to 1.70 bar. This is believed to be due to the reduced gun erosion which occurs for the shorter pump tube. This is likely to be due to the lower maximum temperatures which occur with the shorter pump tube since the initial hydrogen pressure is higher and the total compression ratio is smaller. The muzzle velocities for the high performance shots all run roughly 10 percent below the CFD predicted values. As mentioned above, this is believed to be due to the inadequacy of our simple correction procedure for gun erosion.

We note that, by using the optimized gun operating curve from figure 9 for the shortened pump tube:

- The maximum experimental muzzle velocities were raised from about 7.35 km/sec (for the full length pump tube) to about 8.2 km/sec for the shortened pump tube.

- The maximum velocity of 8.2 km/sec considerably exceeds the all-time previous maximum launch velocity for saboted spheres for this gun—7.4 km/sec (obtained with a full length pump tube).

We now discuss the reduction in gun erosion achieved through the present optimization process. In figure 12 we show the gun erosion, in calibers/shots, for the seven shots for which muzzle velocity data is given in figure 11 and for 12 shots made in the 1960s. We have added trend lines for the old data and two groupings of the new data with the full length and the shortened pump tube. We note that virtually no changes have been made in the gun operating parameters from the 1960s data shown here up until the present optimization effort. The 1960s data shown in figure 12 is virtually the only good data available for the Ames 0.5" gun that was taken previous to the

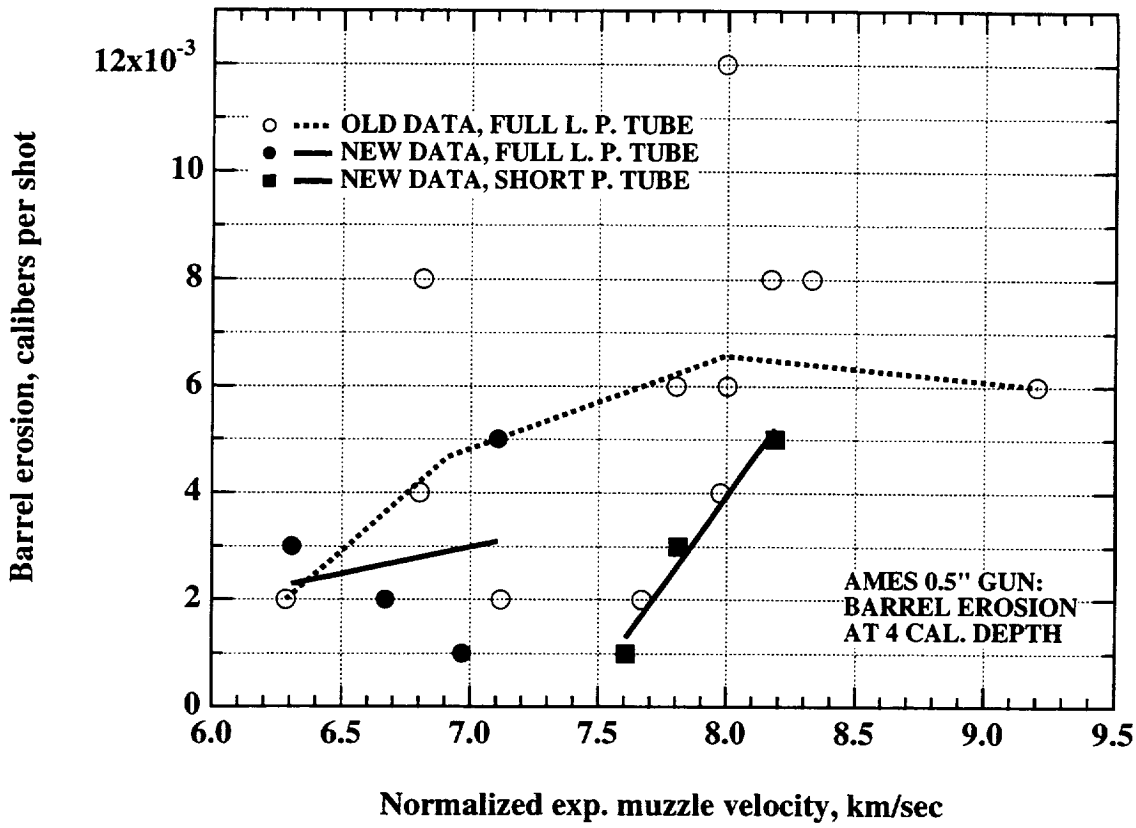

Figure 12. Experimental erosion (calibers/shot) for the Ames 0.5" gun for old 1960s data and for the seven recent shots shown in figure 11. The gun erosion is measured at 4 calibers depth in the barrel. "Full L.P. Tube" denotes full length pump tube and "Short P. Tube" denotes the shortened pump tube.

1990s and with gun operating parameters anywhere near those of the current optimization survey. All gun erosion data is taken at about 4 calibers depth in the barrel. The projectile mass for the seven recent shots varied between 1.17 and 1.35 gm, the average being 1.26 gm. To allow for the variation in projectile mass for the various shots, the muzzle velocities were normalized, on a kinetic energy basis, to a projectile mass of 1.26 gm. That is, if the true muzzle velocity of a 1.17 gm projectile was 8 km/sec, its normalized muzzle velocity would be $(1.17/1.26)^{0.5} \times 8 = 7.71$ km/sec. The normalized muzzle velocity is the ordinate in figure 12. The same normalization procedure was followed for the 1960s data, for which the projectile mass varied from 0.89 to 1.93 gm.

All of the seven recent shots were made operating the gun at conditions close to one or the other of the optimized curves shown in figure 10. The 1960s data was taken, on the whole, for conditions much closer to the unoptimized uppermost curve of figure 6. The piston masses for the old data were between 888 and 1115 grams, whereas for the new data, lighter pistons with masses between 707 and 821 grams were used. For some of the low performance 1960s data, powder masses of 175 gm were used, but for most of the higher performance 1960s shots, the powder masses ranged from 200 to 275 grams. Allowing for the difference between the burning rates of the 4198 and 4895 powders, the equivalent 4198 powder load for all of the seven recent shots was 175 grams. The hydrogen fill pressures for most of the 1960s shots were between 1.03 and 1.51 bar, somewhat lower than that for the uppermost curve of figure 6. Of course, only the second set of three recent shots has the benefit of the shortened pump tube. Also, it is interesting to note that for all except one of the 1960s shots, the break valve pressure had the very high value of 1380 bar, whereas for the optimized curves of figure 10, the break valve pressure ranged from 300

to 600 bar. Lower break valve pressures (down to about 300 bar) were used in other series of shots in the 1960s.

The erosion data is very difficult to take and is subject to large scatter as is evident in figure 12. A rough assessment of data accuracy can be made by grouping data for similar (but not identical) shots and giving the mean and the total scatter range for the grouped data. For example, for the old data between 6.8 and 7.1 km/sec, the erosion can be given as $0.0047^{+0.0033}_{-0.0027}$ calibers/shot (three data points). For the old data between 7.6 and 8.4 km/sec, the erosion can be given as $0.0067^{+0.0053}_{-0.0047}$ calibers/shot (seven data points). For all of the new data grouped together, the erosion can be given as $0.0029^{+0.0021}_{-0.0019}$ calibers/shot (seven data points). For the new data with the shortened pump tube, the erosion can be given as $0.003^{+0.002}_{-0.002}$ calibers/shot (three data points). Although it clearly would be better to have data with better statistics, the author believes the data shown in figure 12 is strongly indicative of substantial reductions in gun erosion achieved as a result of the present optimization process. For example, even with the standard length pump tube, one may make an argument for about a factor of 1.5 reduction in gun erosion between the 1960s and the present, optimized gun operating conditions for normalized muzzle velocities between 6.6 and 7.2 km/sec. Comparing the new data with the shortened pump tube with the old data for normalized muzzle velocities between 7.5 and 8.4 km/sec, we see strong evidence for about a factor of 2 reduction in gun erosion achieved as a result of the present optimization process. (We note that, in fig. 12, all of the 1960s shots for which erosion data is shown were made with polycarbonate slugs, whereas all seven of the recent shots for which erosion data is shown were made with saboted spheres.)

From both the muzzle velocity and gun erosion data (figs. 11 and 12), it was concluded that the CFD optimization process was very valuable in obtaining the best performance from the Ames 0.5" gun.

D. Variation of Angle of High Pressure Contraction Cone

All the CFD gun cycle solutions discussed up to this point were made with a high pressure contraction section cone full angle of 12.4 deg, which corresponds to the current gun configuration and the sketch shown in figure 1. For the conditions of the rightmost point on the lower solid curve in figure 9 (for the shortened pump tube), solutions were run for four other cone angles. These altered cone geometries were obtained from that shown in figure 1 by maintaining the position of the small end of the cone (relative to the diaphragm) and then changing the cone angle. Full cone angles of 12.4 (standard), 22, 31, 40, and 60 degrees were investigated. The pressure histories for the hydrogen cell adjacent to the diaphragm (or projectile base after diaphragm rupture) are shown in figure 13. In order to maintain diaphragm rupture on the same wave, the rupture pressures had to be set, for the 5 different cone angles, to 500, 500, 500, 400, and 300 bar, as shown in figure 13. (N.B: each curve in fig. 13 is offset 2×10^9 dy/cm^2 from the one below for clarity.) Thus, the ordinate axis is correct only for the lowest curve. Offsets to the ordinate axis of 2×10^9 to 8×10^9 dy/cm^2 must be applied for the other curves. For all cases in figure 13, diaphragm rupture occurs on the wave between 0.0165 and 0.0166 sec.

The effects of varying the contraction cone angle are as follows. The maximum projectile base pressure is changed only slightly—the variations are only about 9 percent over the complete angle range investigated here. This is also true for the maximum pressures reached in the high pressure contraction section (not shown here) with the largest variation of that maximum pressure being about 16 percent. However, the rise in pressure becomes much smoother as the cone angle is increased. The first three waves, starting with the wave at diaphragm rupture, are only about half as large for a cone angle of 60 deg than for a cone angle of 12.4 deg. This may be beneficial if one is attempting to launch fragile launch packages. The smoother pressure histories for the larger cone angles are due to a reduction in the shock focusing action of the cone as the angle is increased.

With a significantly increased contraction cone angle, there is a concern that, should there be a loss of hydrogen gas before or during the piston stroke, the piston could impact into the steeper cone at excessively high velocities, leading to excessive pressures and possibly, gun failure. With the more traditional contraction cone angles (5–13 deg), there is a better chance that the cone taper itself, without the usual support from the hydrogen pressure, could halt the piston without damage to the gun. However, in this regard, we note that the AEDC 3.3" gun (ref. 3) has been successfully operated with a contraction section cone angle of 40 deg.

A second five-angle study of the effect of the variation of contraction cone angle was carried out for diaphragm rupture one wave later than for the conditions shown in figure 13. (All other conditions for this second study, except, of course, break valve pressure, were as given in fig. 13.) The results of the second study, not shown here, were generally very similar to those for the first angle study, except that reductions in the maximum projectile

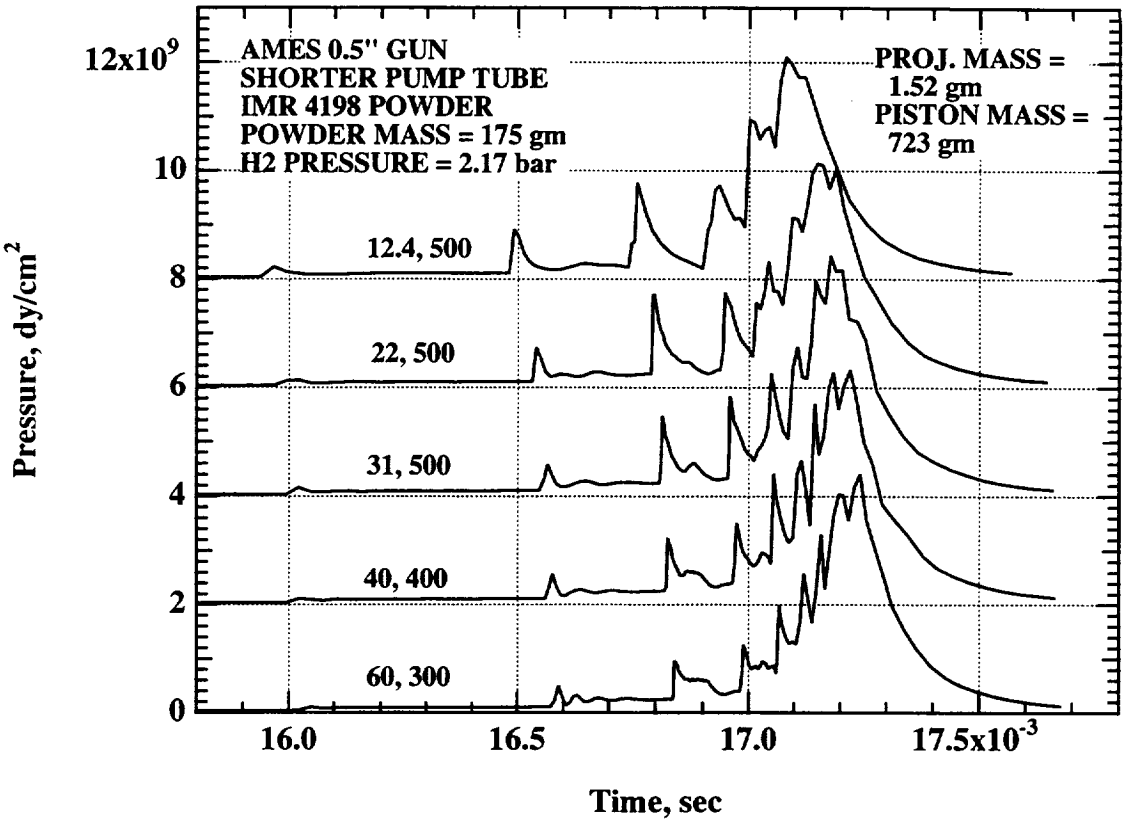

Figure 13. Pressure histories at the hydrogen cell adjacent to the diaphragm (or projectile base) for the five different contraction cone angles. Numbers on curves are contraction cone angle (deg) and break valve rupture pressure (bar). Note that the ordinates are offset 2 x 10^9 dy/cm^2 between curves to separate the curves for clarity.

base pressure up to 15 percent were obtained. The maximum pressure reductions were obtained at a contraction cone angle of 31 deg.

We note that an earlier study (ref. 4) by our group at the NASA Ames Research Center showed a much larger reduction (44 percent) in maximum projectile base pressure as the cone angle in that study was increased from about 9 deg to 60 deg. The different effects of the cone angle variation upon the maximum projectile base pressure are a function of the nature of the pressure history at the projectile base for the baseline (low cone angle) case. For the benchmark projectile base pressure history shown in figure 3 of reference 4, the first and second waves after break valve rupture are very sharply peaked, separated by very deep valleys and are, in fact, the largest two waves. As the cone angle is increased, the peaks are substantially reduced and the intervening valleys partially filled in, leading to substantial reductions in the maximum projectile base pressure. This same effect occurs, as the cone angle is increased, on the first two or three waves after diaphragm rupture shown in figure 13. However, for the gun operating conditions shown in figure 13, these first two or three waves are far from being the highest waves and the region of maximum pressure (at times of 0.0171 to 0.0173 sec) is much smoother, even for the smallest cone angle, and is therefore much less effected by the increase in cone angle. Thus, the effect of the increase of cone angle on the maximum pressure at the projectile base depends very greatly on the nature of the projectile base pressure history for the initial, low cone angle in question.

VI. Summary and Conclusions

Using a well-validated CFD code, a survey of operating conditions of the NASA Ames 0.5" two-stage light gas

gun has been conducted. This survey was aimed at optimizing the performance of this gun. Gun optimization can involve:

1. Increase in muzzle velocity.
2. Reduction in maximum gun pressures.
3. Reduction in maximum projectile base pressure.
4. Reduction in gun erosion.

Seven gun operating parameters were systematically varied during the CFD study. These were powder and piston masses, break valve rupture pressure, initial hydrogen fill pressure, length of pump tube, angle of the high pressure contraction section and projectile mass.

Two main optimizations were performed; the first, for the full length pump tube of the Ames 0.5" gun and the second, for a shortened pump tube with about 40 percent of the pump tube volume removed. Each optimization started with fairly traditional high performance operating conditions for projectiles weighing about 1.5 grams, 900 to 1100 gram pistons, 250 gram powder loads and hydrogen fill pressures of 2.07 and 3.39 bar for the full length and shortened pump tubes, respectively. Each optimization then involved reducing the piston mass to about 720 grams, followed by reducing the powder load to 175 grams, and finally, by reducing the hydrogen fill pressure to 64 percent of its original value. During the optimization procedures, considerable attention was paid to adjusting the break valve rupture pressure, as much as possible, so that rupture would occur on the most favorable wave arriving at the diaphragm just behind the projectile base.

If one compares the new gun operating conditions obtained as the result of these optimizations with the older, more traditional operating conditions, the following predictions can be made. While maintaining a given maximum projectile base pressure, one may raise the muzzle velocity 0.7–0.9 km/sec. One may also choose to maintain the same muzzle velocity and achieve a 30–40 percent drop in maximum projectile base pressure. Further, simultaneously with making either one of these two changes, one should achieve a reduction in gun erosion of 50 percent or more.

A limited experimental verification of these CFD predictions was obtained from a series of seven shots as follows.

1. The maximum experimental muzzle velocities were raised from about 7.35 km/sec for the full length pump tube to about 8.2 km/sec for the shortened pump tube; also, this maximum velocity of 8.2 km/sec considerably exceeds the all-time previous maximum launch velocity of 7.4 km/sec for saboted spheres for this gun (obtained with a full length pump tube).

2. Gun erosion was substantially reduced when compared to similar shots in the past for the Ames 0.5" gun. Gun erosion (at 4 calibers depth) was reduced by about a factor of 1.5 even with the full length pump tube and by a factor of about two for the shortened pump tube. For the latter comparison, the barrel erosion was reduced from about 0.006 calibers/shot to about 0.003 calibers/shot.

Two series of five CFD runs each were made to investigate the effect of varying the contraction section cone angle. Full cone angles of 12.4 deg to 60 deg were investigated in each series. For these two series, the maximum projectile base pressure was found to vary relatively little (15 percent maximum) as the cone angle was varied. However, the pressure rise towards the maximum projectile base pressure became much smoother as the cone angle was increased. This could be important when attempting to launch fragile models. With substantially larger cone angles, there is a concern that, under certain off-nominal conditions, the piston could impact violently into the steeper contraction cone, leading to dangerously high pressures and risking gun failure. Further work would be useful here, particularly with two-dimensional solutions for piston impact into the contraction cone.

References

1. Canning, T. N.; Seiff, A.; and James, C. S.: Ballistic Range Technology. AGARDograph, vol. 138, ch. 2, Aug. 1970, p. 87.
2. Chavez, D. J.; King, C. C.; and Linley, L. L.: A Study to Optimize a 7.6-mm (30-caliber) Two-Stage Light Gas Gun. Presented at the 42nd Aeroballistic Range Association Meeting, Adelaide, South Australia, Oct. 21–25, 1991.
3. DeWitt, J. R.: Configuration Development of the New AEDC 3.3 Inch Launcher. Presented at the 45th Aeroballistic Range Association Meeting, University of Alabama at Huntsville, Ala., Oct. 10–14, 1994.
4. Bogdanoff, D. W.; and Miller, R. J.: Optimization Study of the Ames 1.5" Two-Stage Light Gas Gun. AIAA Paper 96-0099, presented at the 34th AIAA Aerospace Sciences Meeting, Reno, Nev., Jan. 15–18, 1996.

5. Bogdanoff, D. W.; and Miller, R. J.: New Higher-Order Godunov Code for Modelling Performance of Two-Stage Light Gas Guns. NASA TM-110363, Sept. 1995.

6. Bogdanoff, D. W.; and Miller, R. J.: Improving the Performance of Two-Stage Gas Guns by Adding a Diaphragm in the Pump Tub. Presented at the 1994 Hypervelocity Impact Symposium, Santa Fe/Albuquerque, N. Mex., Oct. 16–20, 1994.

7. Bogdanoff, D. W.; and Miller, R. J.: Recent Developments in Gun Operating Techniques at the NASA Ames Ballistic Ranges. To be published as a NASA Technical Memorandum and to be submitted to the 46th Aeroballistic Range Association meeting, Saint-Louis, France, Oct. 14–17, 1996.

REPORT DOCUMENTATION PAGE

Form Approved
OMB No. 0704-0188

1. AGENCY USE ONLY *(Leave blank)*	2. REPORT DATE	3. REPORT TYPE AND DATES COVERED
	March 1996	Technical Memorandum

4. TITLE AND SUBTITLE

Optimization Study of the Ames 0.5" Two-Stage Light Gas Gun

5. FUNDING NUMBERS

478-85-20

6. AUTHOR(S)

D. W. Bogdanoff

7. PERFORMING ORGANIZATION NAME(S) AND ADDRESS(ES)

Thermosciences Institute
Ames Research Center
Moffett Field, CA 94035-1000

8. PERFORMING ORGANIZATION REPORT NUMBER

A-961331

9. SPONSORING/MONITORING AGENCY NAME(S) AND ADDRESS(ES)

National Aeronautics and Space Administration
Washington, DC 20546-0001

10. SPONSORING/MONITORING AGENCY REPORT NUMBER

NASA TM-110386

11. SUPPLEMENTARY NOTES

Point of Contact: D. W. Bogdanoff, Ames Research Center, MS 230-2, Moffett Field, CA 94035-1000
(415) 604-6138

12a. DISTRIBUTION/AVAILABILITY STATEMENT

Unclassified-Unlimited
Subject Category – 12

Available from the NASA Center for AeroSpace Information,
800 Elkridge Landing Road, Linthicum Heights, MD 21090; (301) 621-0390

12b. DISTRIBUTION CODE

13. ABSTRACT ***(Maximum 200 words)***

There is a need for more faithful simulation of space debris impacts on various space vehicles. Space debris impact velocities can range up to 14 km/sec and conventional two-stage light gas guns with moderately heavy saboted projectiles are limited to launch velocities of 7–8 km/sec. Any increases obtained in the launch velocities will result in more faithful simulations of debris impacts. It would also be valuable to reduce the maximum gun and projectile base pressures and the gun barrel erosion rate. In this paper, the results of a computational fluid dynamics (CFD) study designed to optimize the performance of the NASA Ames 0.5" gun by systematically varying seven gun operating parameters are reported. Particularly beneficial effects were predicted to occur if (1) the piston mass was decreased together with the powder mass and the hydrogen fill pressure and (2) the pump tube length was decreased. The optimum set of changes in gun operating conditions were predicted to produce an increase in muzzle velocity of 0.7–1.0 km/sec, simultaneously with a substantial decrease in gun erosion. Preliminary experimental data have validated the code predictions. Velocities of up to 8.2 km/sec with a 0.475 cm diameter saboted aluminum sphere have been obtained, along with large reductions in gun erosion rates.

14. SUBJECT TERMS

Two-stage light gas gun, Space debris impact simulation, Gun erosion studies

15. NUMBER OF PAGES

21

16. PRICE CODE

A03

17. SECURITY CLASSIFICATION OF REPORT	18. SECURITY CLASSIFICATION OF THIS PAGE	19. SECURITY CLASSIFICATION OF ABSTRACT	20. LIMITATION OF ABSTRACT
Unclassified	Unclassified		